



## CYCLIC BEHAVIOR OF CONCRETE FILLED FIBER REINFORCED POLYMER TUBE

Daniel Robillard<sup>1</sup>, Radhouane Masmoudi<sup>2</sup>, and Nathalie Roy<sup>3</sup>

<sup>1</sup> Master Student, University of Sherbrooke, Qc, Canada

<sup>2</sup> PE., Phd, Professor, University of Sherbrooke, Qc, Canada

<sup>3</sup> PE., PhD., Associate Professor, University of Sherbrooke, Qc, Canada

<sup>4</sup> [Radhouane.Masmoudi@USherbrooke.ca](mailto:Radhouane.Masmoudi@USherbrooke.ca)

**Abstract:** Concrete-filled fiber reinforced polymer tubes (CFFT), have been mainly studied under static loading, and very limited research data is available for CFFT columns under cyclic loading. These studies showed the higher structural performance and the relevant use of CFFT for seismic design of reinforced concrete (RC) structures. Indeed, it is well known that CFFT can increase the ductility ratio which is a crucial factor in seismic design. Thus, research on cyclic behavior is essential to the development of new design guidelines using the technology of CFFT. This paper presents the results obtained from an experimental investigation to study the effects of the FRP tube thickness on the cyclic behavior of CFFT columns. Two full-scale CFFT RC columns are reinforced with FRP tube thickness of 4 mm and 8 mm. One control RC column designed according to the Canadian standards for bridges (CSA S6-06) is made for comparison purposes. The specimen setup consisted in a column-footing with the FRP tube embedded in the footing before casting of the concrete. The column is axially loaded under a constant load, while a horizontal hydraulic actuator applied a quasi-static lateral load on the head of the column. The tubes are made at the Composite Material Reinforcement Laboratory of the Sherbrooke University using the filament winding manufacturing process. Comparing the CFFT columns with the control column and also by taking into account for the difference in the concrete sections, we obtain for S0PS2V4 & V8 respectively, 44 % and 46 % more for first cracking moments; 26% and 41% for yielding moments, and 21% and 45% for the ultimate flexural moments. The ductility of CFFT columns are also better than typical RC column with the CFFT specimen reaching 11.38 % and 10.33 % compared to 8.47% for the control.

### 1 Introduction

The use of fiber-reinforced polymer (FRP) in retrofitting old structure has been studied quite extensively during the past two decades. These studies focused primarily on enabling these old ageing reinforced concrete (RC) structures, to upgrade their structural safety performance to meet the requirements of the new national and international codes on seismic design guidelines. They also showed the high potential of use of concrete-filled FRP tube (CFFT) in new structures due to their high durability, their capacity not only to confine concrete but also to act as longitudinal and transverse additional reinforcements. The tube is composed of inclined fibers that gives the needed strength in the transverse direction to confine concrete under axial loading and to resist shear forces under flexural and/or torsion forces. If sufficient longitudinal axial fibers exists, the flexural capacity of the hybrid CFFT column can be enhanced and significant increase in the flexural capacity can be obtained. The design possibilities of these new-hybrid high-performance CFFT structural members are innovative, and has to be studied before full-acceptance by the construction industry.

## **2 Behavior of CFFT**

### **1.1 Static behavior of CFFT**

Extensive research has been made on axial behavior Mohamed and Masmoudi (2010), Mohamed et al. (2010), Wong et al. (2008), Cui et Sheikh (2010), Lim et Ozbakkaloglu (2014), Eid et Paultre (2008). For Flexural behavior of CFFT beams, Fam et al. (2002, 2005), Yu et al. (2006), Abouzied & Masmoudi (2016), studied the effect of different design parameters on the structural performance of CFFT beams. However, very few research studied the interaction between the axial load and the flexural capacities of CFFT columns, Mirmiran et al. (1999) and Nanni et al. (1995). For shear behavior, the performance of CFFT column or beam, can be considered better than conventional RC beams or columns, while being cost effective in terms of installation compared to steel stirrups. The CSA S806-12 gives the different provision regarding the shear resistance of FRP-externally confined columns. The Japanese code JSCE (2001) noted that North American codes treat axial and transverse FRP reinforcements in separate sections and equations, which is not the case in the Japanese code, where these two aspects are both considered at the same time in one equation from JSCE (1997).

### **1.2 Cyclic behavior of CFFT**

One of the best application of CFFT structural members is a beam-column system acting as the seismic force resistance system (SFRS). Typical reinforced concrete (RC) column in either a building or bridge when subjected to an earthquake will lose a portion of their concrete section leading to a reduction of their stiffness and structural integrity, and a lot of damage in the plastic hinge in the form of crushed concrete. Whereas CFFT columns keep their section integrity in keeping the concrete section and due to the expansion of concrete a mechanism of passive confinement takes place enhancing the concrete strength. CFFT column are known to reach higher ductility than RC column for the same limit state as shown in Jean et al. (2012). This advantage of CFFT column is particularly interesting for high seismic activity zones; meaning reduced damage by low to medium earthquakes leading to better economic sustainability in these zones. Research on cyclic behavior of CFFT columns have been made by Ozbakkaloglu et Saatcioglu (2004), Shao et Mirmiran (2005), Ozbakkaloglu et Saatcioglu (2006, 2007), Idris et Ozbakkaloglu (2013) and Ozbakkaloglu et Idris (2014). Considering that most new building usually have a RC shear walls acting as the major SFRS instead of beam-column system it is less desirable for engineers to use CFFT elements in building apart for highly exposed columns to environmental factors like outdoor tiered parking where CFFT use should be highly sought. One of the best use of CFFT columns is in bridge where they act as the major SFRS. Multiple studies has been made on these type of column Zhu et al. (2006), Saatcioglu et al. (2008), Zohrevand et Mirmiran (2012, 2013), Zaghi et al. (2012), Youm et al. (2013). Some of these studies use high strength concrete (55+ and 100+ MPa) wich is less desirable for engineers considering the cost of such concrete in massive volume.

## **3 Research project**

This paper presents the results of three full-scale specimens, while additional full-scale test results are ongoing.

### **3.1 Experimental Program**

#### **3.1.1 Specimen and loading description**

Cyclic tests are conducted on two full-scale CFFT columns and one conventional RC column for comparison purposes. This RC column is reinforced in shear with steel spiral stirrups. Both CFFT columns are reinforced with GFRP tubes having stacking sequences of  $(90/\pm 65/90)$  and  $(90/\pm 65/90)_2$  giving an approximate tube thickness of 4 and 8 mm, respectively. The columns are 2 m-high, with a concrete core diameter of 305 for the control and 324 mm for the two CFFT column. The FRP tubes are embedded (embedment length of  $1.23 D$ , where  $d$  is the diameter of the column) into a strong RC concrete footing, which is directly anchored to a strong structural slab. The axial load is applied by two Dywidag high strength bars, using Enerpac load-cells to control the axial load level. A force of 145 kN per bar is applied giving approximately 10% to 15% of  $f'_c$  in axial load; which is typical of bridge structure. A 250 kN servo-hydraulic actuator is used to apply the lateral cyclic loading, while being fixed to a large reaction RC wall. The first cycle of loading consist of applying 75 % of the expected yield load. The second cycle is to apply the load until the steel rebar reach their yielding point. The subsequent cycles are repeated twice with a maximum displacement of 1.5, 2, 3,... times the yield displacement up to failure. Table 3.1 provides the characteristics of each column, whereas

Tables 3.2 presents the properties of the concrete and steel; and Table 3.3 shows the mechanical properties of the FRP tubes used in this project. Figure 3.1 shows the specimen and test-Setup during testing.



**Figure 3.1:** From left to right, specimen S75PS2V0, S0PS2V4 and S0PS2V8

**Table 3.1:** Specimen description

Column	Concrete core Diameter (mm)	Fiber type	FRP tube thickness (mm)	Longitudinal Reinforcement	Transverse Reinforcement
S75PS2V0	305	None	None	8 – 15M	10 M @ 75 mm c/c
S0PS2V4	324	Glass	4	8 – 15M	None
S0PS2V8	324	Glass	8	8 – 15M	None

**Table 3.2:** Concrete and steel properties

	$f_c$ (MPa)	$f_{tc}$ (MPa)	$E_c$ (MPa)	$f_{y\_long}$ (MPa)	$f_{y\_trans}$ (MPa)
S75PS2V0	35.19	3.67	22.36		460
S0PS2V4	32.69	3.52	20.75	430	N/A
S0PS2V8	32.24	4.00	18.82		N/A

**Table 3.3:** GFRP tube properties

GFRP Tube	Compression		Long. Tension		Trans. Tension*	
	$f_{FRP}$ (MPa)	$E_{FRP}$ (GPa)	$f_{FRP}$ (MPa)	$E_{FRP}$ (GPa)	$f_{FRP}$ (MPa)	$E_{FRP}$ (GPa)
GFRP Tube	65	13.5	15.5	6.56	505	16.00

\*Obtained from 6'' FRP ring, further test with full-scale FRP ring will be made

### 3.1.2 Instrumentation

Each column is instrumented with 16 strain gages bonded on the steel bars and distributed from -200 mm (in concrete footing) to +600 mm of the interface between the footing and the column. These strain gages are to monitor the steel strains during the tests, where six of them helped to determine the yield strains and load during the second run of the same cycle of loading. The specimens are also equipped with two metal rings at 50 mm and 500 mm from the base

interface to monitor the rotations in the plastic hinge. One of the constraint in this project is to keep the tube integrity to its maximum, so no local holes in the tube is allowed, particularly in the plastic hinge zone. Therefore, the rings are tied and squeezed to the column as shown in Figure 3.2. Four horizontal potentiometers at 125, 225, 325, 425 mm from the footing are used to monitor the displacement in the plastic hinge. One potentiometer is placed at 2045 mm from the top face of the footing, at the same elevation of the lateral force applied by the servo-hydraulic actuator, is used to monitor the maximum-tip displacement of the CFFT column. Acoustic-emission sensors are placed all over the columns to capture the noise caused by concrete cracking. This non-destructive method is used to evaluate the progressive damage in the concrete. Finally, 18 strain gages are bonded on the FRP tube to monitor the strains in the FRP tube. Figure 3.2 shows the instrumentation in the plastic hinge zone.

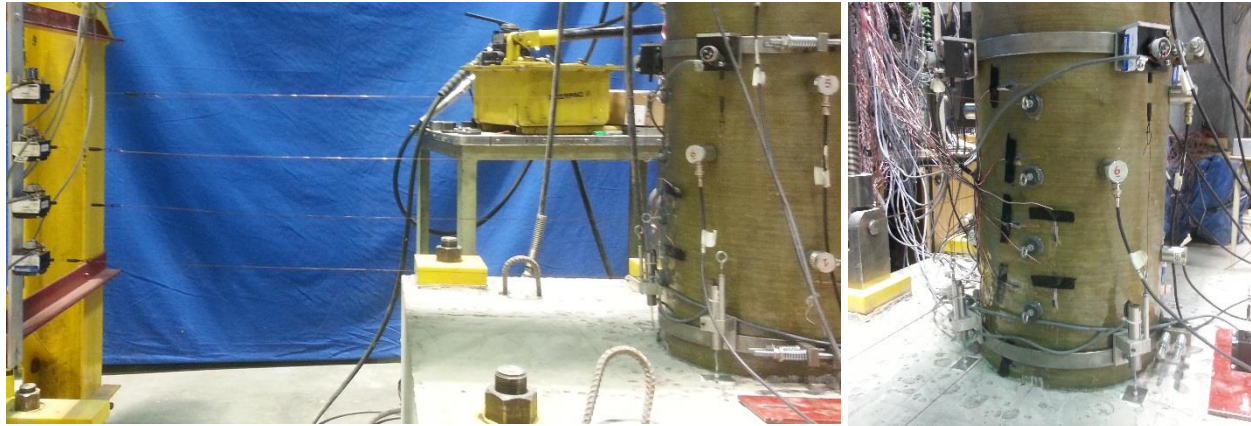


**Figure 3.2:** Instrumentation in the plastic hinge of the column (West side of the column)

## 3.2 EXPERIMENTAL RESULTS

The results of all specimens are shown in Figures 3.3 to 3.5 with a brief discussion for each test. The results are presented in the form of a load-displacement curve where the displacement is converted into percentage of the drift.

### 3.2.1 S75PS2V0 control RC column

Figure 3.3 shows the results obtained from the control column, which is a typical RC column. The control column is considered failed after it had lost more than 20 % of its maximum applied load. Rupture of the column was due to the excessive crushing of the concrete in the plastic hinge. The maximum applied load was 48.4 kN at 2.10% drift in the positive direction and 55.1 kN at 2.09% drift in the negative direction. The failure happened in the negative direction where we reached less than 20% of the maximum value in that direction. The maximum drift ratio of the control column was 8.47% in the positive direction and 8.18% in the negative direction. During positive and negative loadings, the side under compression is respectively the west and east sides Figures 3.3 b) and c) show the west and east sides of the column after all crushed concrete was removed. We can see the extent of the damage on each side of the column. The height of the damage reaches approximately 250 mm (0.82D) for the east side and 300 mm (0.98D) for the west side of the column.

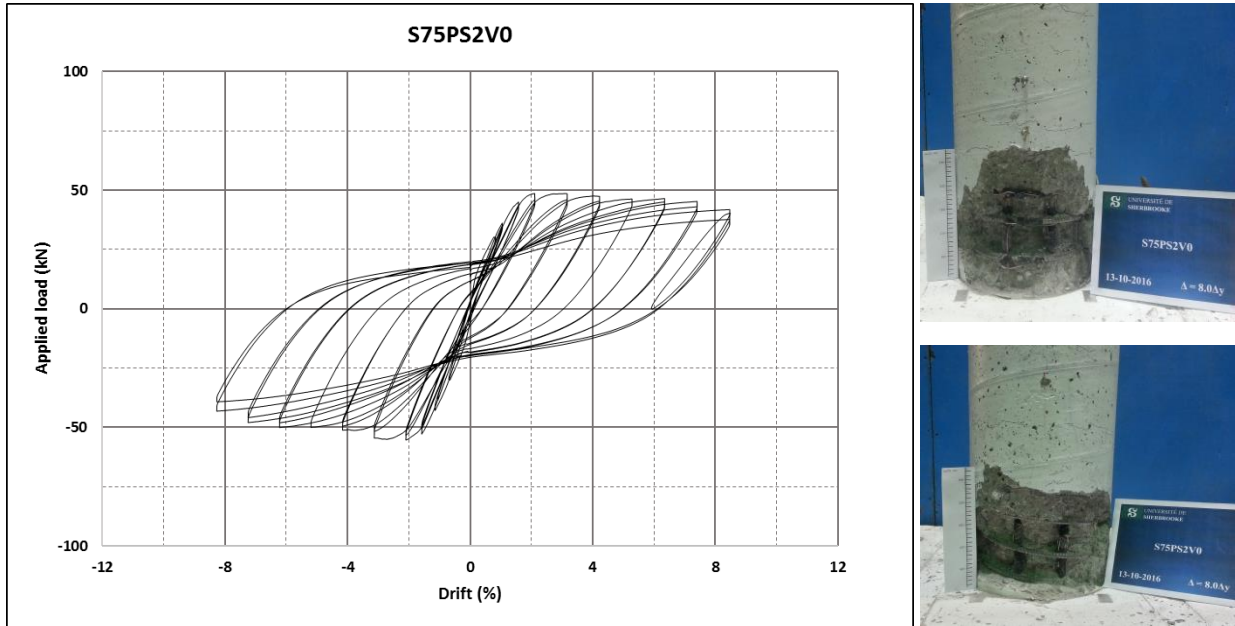


**Figure 3.3:** Control Specimen S75PS2V0 a) Load displacement curve b) (Up) West side c) (Down) East side

### 3.2.2 S0PS2V4 4 mm- FRP Tube CFFT column

Figure 3.4 shows the results obtained from the CFFT column with 4 mm FRP tube thickness. The specimen S0PS2V4 was considered failed after the total rupture of one of its steel rebar. Rupture of the column first happened in the negative direction during the first cycle with 10 times the yield displacement ( $\Delta y$ ). The test was continued to finish the second cycle in the positive direction where a second steel rebar ruptured. Rupture in the longitudinal direction of the most strained fibers started at the end of  $3\Delta y$  and complete rupture in this direction was noted at  $5\Delta y$ . Buckling in compression of the FRP tube on the west side of the column was observed at  $9\Delta y$  at a height of 125 mm from the foundation. The maximum applied load was 68.0 kN at 8.94% drift in the positive direction and 70.0 kN at 10.24% drift in the negative direction. The maximum drift ratio of the column was 11.16% in the positive direction and 11.38% in the negative direction. Figure 3.4 b) and c) show the extent of the damage on each side. After removing the FRP tube from the column in the plastic hinge the amount of damage was minimal apart in the small zone between 0 to 50 mm of the foundation. The cracked concrete had to be removed using a hammer due to a better compacted concrete in the plastic hinge, compared to the RC specimen. The height of the damage ranged between 150 mm to 250 mm at the highest point (0.46D to 0.77D) for the west side and 200 mm (0.62D) for the east side. The thickness of the loose concrete removed was less than an inch (25 mm) apart from the zone between 0 to 50 mm from the foundation.

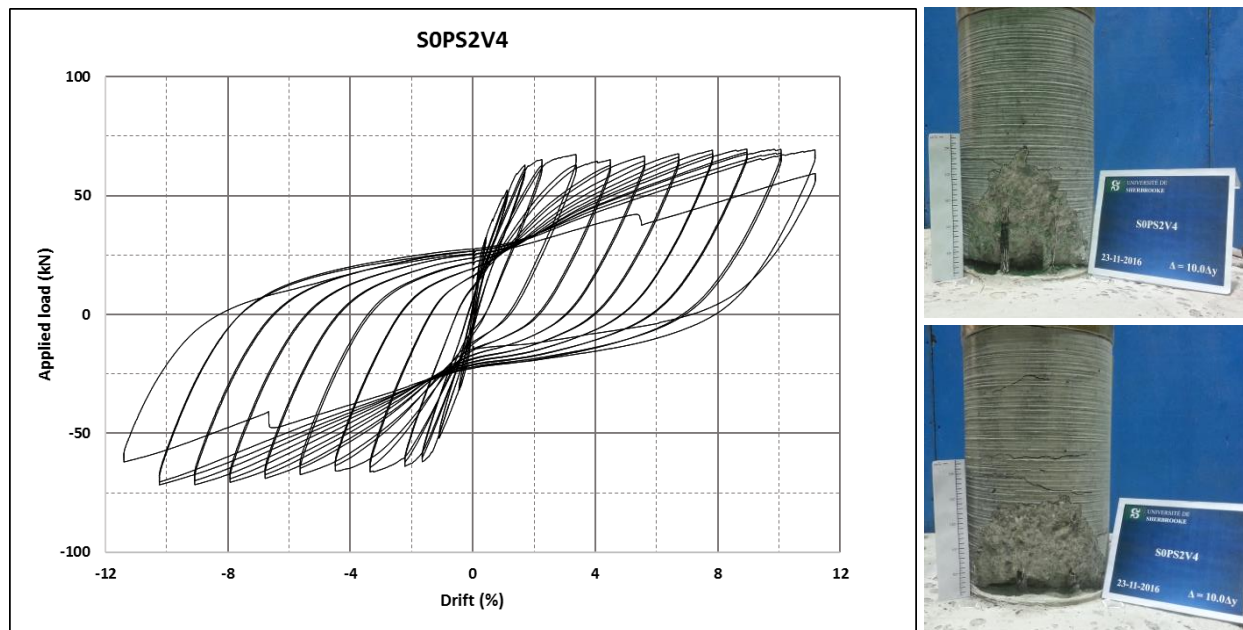


**Figure 3.4:** CFFT Specimen S0PS2V4 a) Load displacement curve b) (Up) West side c) (Down) East side

### 3.2.3 S0PS2V8 8 mm-FRP Tube-CFFT column

Figure 3.5 shows the results obtained from the column with 8 mm FRP tube thickness. The test on specimen S0PS2V8 was abruptly stopped at a drift of  $8\Delta y$  due to failure of one of the Dywidag bars. The rupture caused a partial rupture of the column head, bending of the fixation rod. Minor spalling of the concrete was observed on the foundation at  $3\Delta y$  on the west side. Rupture in the longitudinal direction of the most strained fibers started at  $5\Delta y$  and complete rupture in this direction was noted around  $7\Delta y$ . The maximum applied load reaches 82.4 kN at 5.61% drift in the positive direction and 77.3 kN at 4.52% drift in the negative direction. The maximum drift ratio of the column was 10.02 % in the positive direction and 10.33 % in the negative direction. Figure 3.5 b) and c) show the extent of the damage on each side. After removing the FRP tube from the column in the plastic hinge, the amount of damage was minimal and limited in a zone between 0 to 50 mm from the top foundation level. The height of the damage is 175 mm at the highest point (0.54D) for the west side and 200 mm (0.62D) for the east side. The thickness of the loose concrete was even less than the specimen S0PS2V4.

Table 3.4 resume the results obtained for each specimen and Figure 3.6 shows the load-drift envelope of each specimen for comparison purposes.

**Table 3.4 :** Result summary

	$M_{cr}$ (kNm)	$M_y$ (kNm)	$M_{ult}$ (kNm)	Max Drift (%)
S75PS2V0	26.58	80.54	112.62	8.47
S0PS2V4	40.09	106.55	143.17	11.38
S0PS2V8	40.09	117.56	168.53	10.33

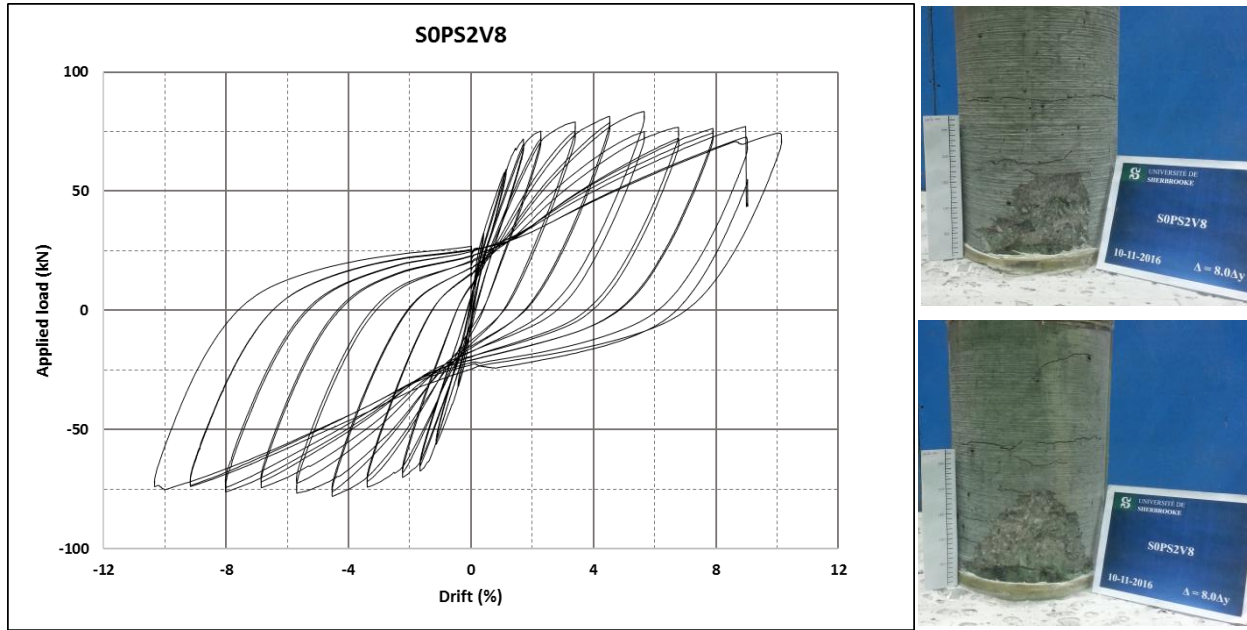


Figure 3.5: SOPS2V8 a) Load displacement curve b) (Up) West side c) (Down) East side

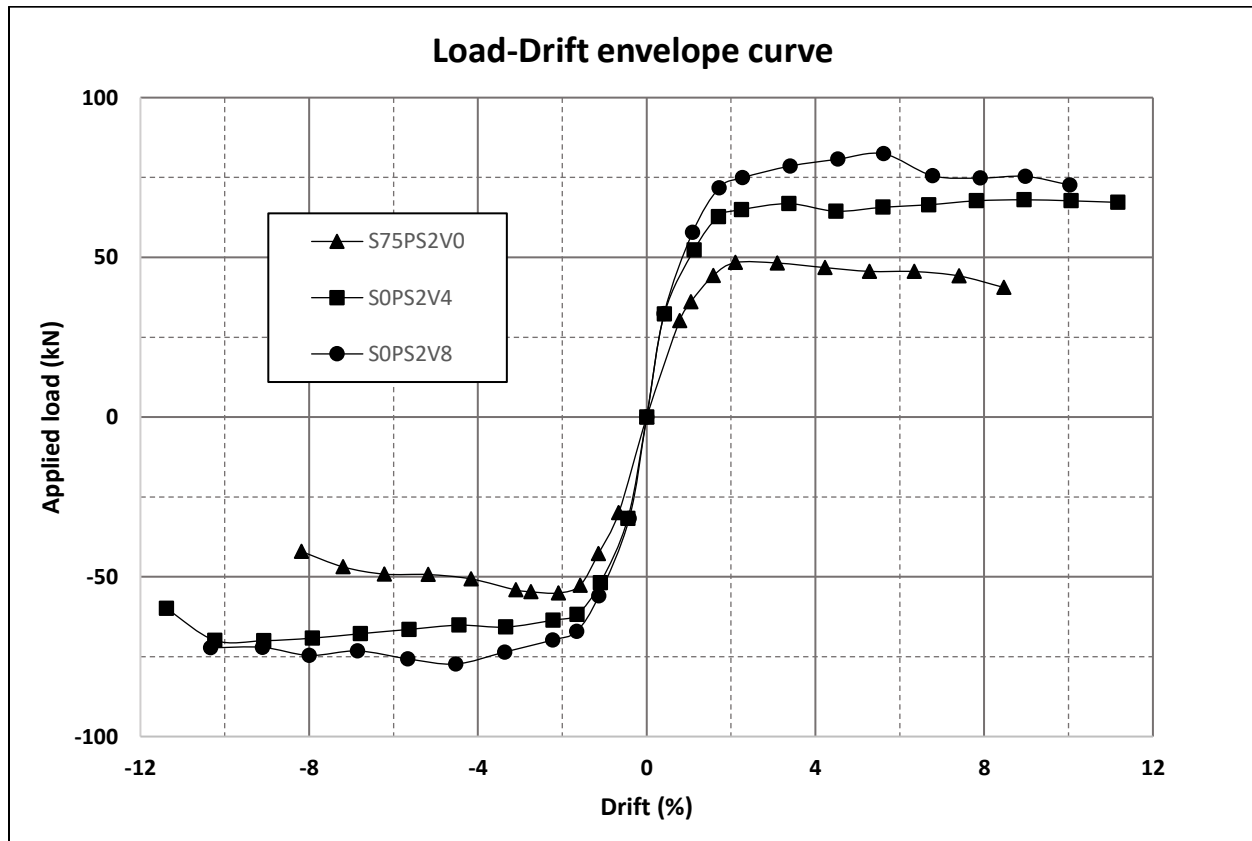


Figure 3.6: Load-Drift envelope curve of the tree specimen

## **4. Discussion**

### **4.1 Limit state**

The typical limit state of a typical RC column is chronologically under cyclic loading is described as: 1) the cracking of the concrete cover; 2) the yielding of the steel longitudinal reinforcement; 3) The spalling and crushing of the concrete core and finally 4) the buckling of the longitudinal steel reinforcement. The limit state of the control specimen was the same, as described above, with the rupture occurring due to the extensive damage in the plastic hinge. The loss of the concrete section due to crushing and spalling and buckling of the steel rebar led to the complete failure of the column in the plastic hinge zone. For the CFFT columns, the limit state can be chronologically described as: 1) the cracking of the concrete; 2) the yielding of the steel longitudinal reinforcement; 3) the failure of the FRP tube in the longitudinal direction in the tension side; 4) the local buckling of the FRP tube in compression for the small-thickness tube; and finally 5) Total rupture of the longitudinal steel reinforcement leading to the column failure. If we compare both CFFT columns, we can deduce that the thicker tube (SOPS2V8) enables the column to reach a higher lateral loading but also prevent the local buckling of the FRP tube in compression. Furthermore, the complete failure of the FRP in the longitudinal direction happens later with specimen SOPS2V8 at a drift ratio of 5.61% versus 3.37% with the thinner tube (SOPS2V4). It is interesting to note that the strength of specimen SOPS2V8 gradually comes closer to the strength of specimen SOPSV4. A fact that is expected due to the complete failure of the FRP in the longitudinal direction.

### **4.2 Strength, ductility and durability**

The strength of the CFFT columns is by far stronger than the typical RC column as shown by the above results. When comparing the CFFT columns with the control column and also by taking into account for the difference in the concrete sections, we obtain for SOPS2V4 & V8 respectively, 44 % and 46 % more first cracking moments; 26% and 41% for yielding moments, and 21% and 45% for the ultimate flexural moments. The ductility of CFFT columns are also better than typical RC column with the CFFT specimen reaching 11.38 % and 10.33 % compared to 8.47% for the control. The drift ratio of the thicker tube is supposed equal or higher to the one thinner. Thus the CFFT columns drift ratio are 34 % higher than the control column. This difference is explained by the failure mode, which is from the rupture of the longitudinal steel reinforcement compared to the crushing of concrete for the RC column. This behavior explains the absence of notable loss in strength under high displacement compared to the RC column, where we can see a notable reduction in strength. These great gains in strength and ductility enhance the quantity of energy ready to be dissipated during an earthquake giving higher structural response to seismic loads. The durability of concrete structure is directly dependant on the presence of cracks, which gives the opportunity for water to infiltrate. Concrete cracks appear due to shrinkage and loading, which appear as soon as  $M_{cr}$  is reached. As for the CFFT column, the concrete is protected till the FRP starts failing in the longitudinal direction. In the specimen SOPS2V4 & V8 the tube stops protecting the concrete at 3.36% drift ( $3\Delta y$ ) and 5.61% ( $5\Delta y$ ) respectively. The FRP Tubes protect the concrete against aggressive environments even after low to moderate earthquakes. Thus, CFFT columns can be cost effective.

## **5. CONCLUSION**

CFFT columns enhanced the ultimate strength and maximum drift ratio compared to typical RC column. They also present little loss of strength and reduced damage at high displacement. Moreover, they change the failure mode to rupture of the longitudinal steel reinforcement instead of crushing of the concrete core, which leads to the buckling of the steel rebar. Their durability is high due to the late rupture of the tube in the longitudinal direction preventing any infiltration making it possible to keep the concrete protected even during low to moderate earthquakes. To design CFFT columns, we need to choose the concrete section and strength, the tube properties and the longitudinal steel reinforcement. Analysis and the development of design equations are ongoing and will be presented in future publications.

## **ACKNOWLEDGEMENTS**

The reported research in this paper is sponsored by the Natural Sciences and Engineering Research Council of Canada (NSERC). The authors also acknowledge the contribution of the Canadian Foundation for Innovation (CFI) for the



infrastructure used to conduct testing. The technician Claude Aubé was responsible for the preparation of the Test-Setup.

## REFERENCES

- Mohamed, H. M., Abdel-Baky, H. et Masmoudi, R. (2010). Nonlinear stability analysis of concrete-filled fiberReinforced polymer-tube columns: Experimental and theoretical investigation. *ACI Structural Journal*, volume 107, numéro 6, p. 699-708.
- Mohamed, H. M. and Masmoudi, R. (2010). Axial load capacity of concrete-filled FRP tube columns: Experimental versus theoretical predictions. *Journal of Composites for Construction*, volume 14, numéro 2, p. 231-243.
- Wong, Y. L., Yu, T., Teng, J. G. et Dong, S. L. (2008). Behavior of FRP-confined concrete in annular section columns. *Composites Part B: Engineering*, volume 39, numéro 3, p. 451-466.
- Cui, C., and Sheikh, S. A. (2010). "Analytical model for circular normal and high-strength concrete columns confined with FRP." *J. Compos. Constr.*, 10.1061/(ASCE)CC.1943-5614.0000115, 562–572.
- Lim, J. C. et Ozbakkaloglu, T. (2014). Confinement Model for FRP-Confined High-Strength Concrete. *Journal of Composites for Construction*, volume 18, numéro 4, p. 04013058 (19 pp.).
- Eid, R. and Paultre, P. (2008). "Analytical Model for FRP-Confined Circular Reinforced Concrete Columns." *J. Compos. Constr.*, 12(5), 541–552.
- Fam, A. Z. et Rizkalla, S. H. (2002). Flexural behavior of concrete-filled fiber-reinforced polymer circular tubes. *Journal of Composites for Construction*, volume 6, numéro 2, p. 123-132.
- Fam, A., Schnerch, D. et Rizkalla, S. (2005). Rectangular filament-wound glass fiber reinforced polymer tubes filled with concrete under flexural and axial loading: Experimental investigation. *Journal of Composites for Construction*, volume 9, numéro 1, p. 25-33.
- Yu, T., Wong, Y. L., Teng, J. G., Dong, S. L. et Lam, E. S. S. (2006). Flexural behavior of hybrid FRP-concrete-steel double-skin tubular members. *Journal of Composites for Construction*, volume 10, numéro 5, p. 443-452.
- Mirmiran, A., Shahawy, M. et Samaan, M. (1999). Strength and ductility of Hybrid FRP-concrete beam-columns. *Journal of Structural Engineering*, volume 125, numéro 10, p. 1085-1093.
- Nanni, A. et Norris, M. S. (1995). FRP jacketed concrete under flexure and combined flexure-compression. *Construction and Building Materials*, volume 9, numéro 5, p. 273-281.
- JSCE (2001), Recommendation for upgrading of concrete structures with use of continuous fiber sheets, *Concrete Engineering Series 41*, Japan Society of Civil Engineers, Tokyo
- JSCE (1997), Recommendation for design and construction of concrete structures using continuous fiber sheets, *Concrete Engineering Series 23*, Japan Society of Civil Engineers, Tokyo
- Jean, M., St-Martin, C., Roy, N., Rivard, P., Moradian, Z., Carvalho, E., Proulx, J. (2012), Limit states of reinforced concrete bridge piers confined with carbon fiber reinforced polymer (CFRP), 15th WCEE, Lisboa 2012, University of Sherbrooke, Canada
- Ozbakkaloglu, T., et Saatcioglu, M. (2004). Seismic performance of High-Strength concrete columns cast in stay-in-place FRP formwork, 13th WCEE, University of Ottawa, Canada

- Shao, Y. et Mirmiran, A. (2005). Experimental investigation of cyclic behavior of concrete-filled fiber reinforced polymer tubes. *Journal of Composites for Construction*, volume 9, numéro 3, p. 263-273.
- Ozbakkaloglu, T. et Saatcioglu, M. (2006). Seismic behavior of high-strength concrete columns confined by fiber-reinforced polymer tubes. *Journal of Composites for Construction*, volume 10, numéro 6, p. 538-549.
- Ozbakkaloglu, T. et Saatcioglu, M. (2007). Seismic performance of square high-strength concrete columns in FRP stay-in-place formwork. *Journal of Structural Engineering*, volume 133, numéro 1, p. 44-56.
- Idris, Y. et Ozbakkaloglu, T. (2013). Seismic behavior of high-strength concrete-filled FRP tube columns. *Journal of Composites for construction*, volume 17, numéro 6, p. 04013013 (13 pp.).
- Ozbakkaloglu, T. et Idris, Y. (2014). Seismic Behavior of FRP-High-Strength Concrete-Steel Double-Skin Tubular Columns. *Journal of Structural Engineering*, volume 140, numéro 6, p. 04014019 (14 pp.).
- Zhu, Z., Ahmad, I. et Mirmiran, A. (2006). Seismic performance of concrete-filled FRP tube columns for bridge substructure. *Journal of Bridge Engineering*, volume 11, numéro 3, p. 359-370.
- Saatcioglu, M., Ozbakkaloglu, T. et Elnabesy, G. (2008). Seismic behavior and design of reinforced concrete columns confined with FRP stay-in-place formwork. Dans *FRP Stay-in-Place Forms for Concrete Structures Sessions - ACI Spring Convention 2008, March 31, 2008 - March 31*. American Concrete Institute, Los Angeles, CA, United states, p. 145-165.
- Zohrevand, P. et Mirmiran, A. (2012). Cyclic behavior of hybrid columns made of ultra-high performance concrete and fiber reinforced polymers. *Journal of Composites for Construction*, volume 16, numéro 1, p. 91-99
- Zohrevand, P. et Mirmiran, A. (2013). Effect of column parameters on cyclic behavior of ultra-high performance concrete filled fiber reinforced polymer tubes. *ACI Structural Journal*, volume 110, numéro 5, p. 823 – 831
- Zaghi, A. E., Saiidi, M. S. et Mirmiran, A. (2012). Shake table response and analysis of a concrete-filled FRP tube bridge column. *Composite Structures*, volume 94, numéro 5, p. 1564-74
- Youm, K., Cho, J., Lee, Y. et Kim, J. J. (2013). Seismic performance of modular columns made of concrete filled FRP tubes. *Engineering Structures*, volume 57, p. 37-50.